DAILY PERFORMANCE OF A SOLAR DISH COLLECTOR

by

Saša R. PAVLOVIĆ[a*], Velimir P. STEFANOVIĆ[a], Žarko M. JANKOVIĆ[c], Evangelos BELLOS[b], and Darko M. VASILJEVIĆ[d]

[a] Department of Energetics and Process technique, Faculty of Mechanical Engineering, University in Nis, Nis, Serbia
[b] Department of Thermal Engineering, National Technical University of Athens, Athens, Greece
[c] Faculty of Occupational Safety, University of Nis, Nis, Serbia
[d] Photonics Center, Institute of Physics, University of Belgrade, Belgrade, Serbia

Original scientific paper
https://doi.org/10.2298/TSCI180124098P

Solar energy exploitation is one of the most promising techniques for achieving the sustainability in the energy domain. The objective of this work is to investigate the daily performance of a solar dish collector under different operating temperature levels. A solar dish collector with 10.28 m^2 aperture and a spiral coil absorber is investigated. The analysis is performed with a developed numerical model in engineering equation solver which has been validated with experimental results. The analysis proved that the daily thermal efficiency of the collector is ranged from 67.36% to 54.65% for inlet temperatures from 50 °C to 350 °C, respectively. On the other hand, the exergy efficiency presents an increasing rate of the inlet temperature and it is found to be ranged from 8.77% up to 31.07% for the respective temperatures. The daily exergy production of the collector can reach up to 26 kWh with a respective thermal production of 50 kWh for inlet temperature equal to 350 °C. The results of this work can be exploited for the suitable evaluation of the solar dish collector on a daily basis.

Key words: *solar dish collector, daily performance, thermal analysis, exergy analysis*

Introduction

Solar energy utilization is an important weapon for facing numerous problems as the global warming, the fossil fuel depletion and the high price of electricity. Solar concentrating technologies are promising solutions for producing heat at medium and high temperatures [1, 2]. Numerous applications as desalination, space-heating, space-cooling, industrial heat, power production, and chemical processes can utilize the solar energy. The most usual concentrating technologies are the parabolic trough collector, the linear Fresnel collectors, the solar dishes and the solar towers [3, 4]. Among these technologies, the solar dishes are a developing technology and a lot of research has been focused on them for two reasons. Firstly, these are compact systems which can be installed in many places and in roofs of building for example and they can produce heat at high temperatures because of they concentrate the solar irradiation a very small region [5].

* Corresponding author, e-mail: saledoca@gmail.com

In the literature, there are many configurations of solar dish collectors which present different advantages and disadvantages. Loni *et al.* [6] examined a cylindrical receiver in a solar dish collector for feeding an ORC with the heat. They optimized their cavity by determining the optimum shape of the cylindrical cavity. They found that there is an optimum aperture diameter which maximizes the thermal efficiency of the collector. Moreover, Zou *et al.* [7] also found the existence of an optimum diameter of the cylindrical cavity receiver. Furthermore, Mawire and Taole [8] examined a cylindrical cavity solar dish collector with 52% optical efficiency which presents total thermal loss coefficient close to 4.6 W/m.

In the literature, there are many studies which investigate alternative cavities. The square prismatic tubular cavity and the hemispherical cavity receiver have been examined by Loni *et al.* [9, 10]. Xu *et al.* [11] investigated an innovative tapered tube bundle receiver in order to achieve uniform heat flux and to operate at high temperatures (~1000 K). A pressurized volumetric receiver has been studied by Zhu *et al.* [12] and it is found to have maximum exergy efficiency close to 36%. A comparative study has been carried out by Daabo *et al.* [13] where the cylindrical, conical and spherical receivers are compared. According to their results, the conical receiver is the best case among the examined. Moreover, it is important that there is a plenty of literature studies which investigate different ideas with solar dish collectors. The use of a solar dish collector in a Rankine cycle has been examined by Loni *et al.* [14], while the use of nanofluids as working fluids in solar dishes has been examined in [15]. Moreover, the artificial neural network has been used for the prediction of the solar dish performance in [16].

Alternative absorber geometry is the spiral coil geometry which has been examined by Pavlovic *et al.* [17, 18], Stefanović *et al.* [19], and Pavlović *et al*. [20-22] experimentally and numerically. This absorber coil is located inside a housing and it is a low-cost and flexible system. In the previous literature studies, the instantaneous efficiency of this system has been examined. The objective of this work is to determine the daily performance of this collector in order to know the daily energy and exergy potential of this system for operation at different temperature levels. In the literature, there is lack of studies about the daily performance of solar concentrating technologies and especially of solar dish collectors. So, this study is able to give important results and conclusions for the sustainability of these systems. The knowledge of the daily performance of the solar dish collectors is crucial in order to decide the applications in which these systems have to be used. Moreover, the parametric analysis of the present work gives results in this direction.

Material and methods

The examined solar collector

The examined solar dish collector is depicted in fig. 1. This figure shows all the system and it includes an extra region with the spiral absorber. The total aperture of the collector is about 10.29 m^2 and the concentration ratio is 28.26. This collector has been examined experimentally and numerically in previous papers [17-22] and more details about this collector can be found on these references. There is no reason for giving again all the details in this work.

This collector had presented reduced optical efficiency in the previous studies because of the low-quality reflective material (PMMA-Polymethyl methacrylate) which has a reflectance close to 60%. In this study, the use of an improved material (Vega WR193) with 90% reflectance [23] is performed. So, the estimated optical efficiency of the system will reach up to 69%, using 80% absorbance [18] and 96% intercept factor [22]. In other words:

$$\eta_{\text{opt}} = \rho\gamma\alpha = 0.9 \cdot 0.96 \cdot 0.8 \approx 0.69 \quad (1)$$

So, this improvement is applied in the present work in order to estimate the daily performance of the improved system. The optical efficiency of 69% is a satisfying value which can lead to a sustainable design. The analysis is performed with a developed model in engineering equation solver (EES) [24]. This model has been described with all the proper details in [17-19] and so there is no reason for giving the same modeling again. Moreover, the validation of this model with the experimental results has been given in these references. In this work, the examined working fluid is Therminol VP-1 [25] which is able to operate from 12 °C up to 400 °C with a safety.

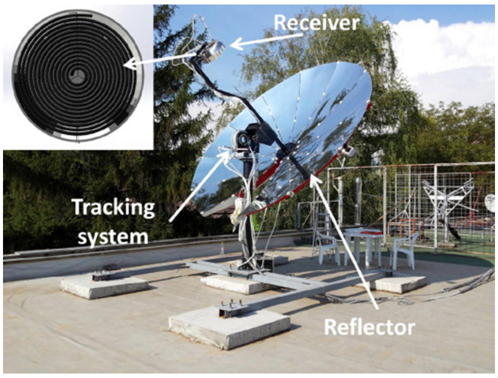

Figure 1. The examined solar dish collector [18]

Mathematical formulation

In this subsection, the basic equations for the evaluation of the obtained results are given. These equations are associated with the energy and exergy efficiency calculations. The exergy analysis is very important for the concentrating technologies because they are able to operate in high temperature level and in power production applications.

The useful heat production, Q_u, is calculated using the energy balance in the fluid volume.

$$Q_u = \dot{m}c_p\left(T_{out} - T_{in}\right) \tag{2}$$

The solar energy, Q_s, is calculated using the incident solar beam irradiation:

$$Q_s = A_a G_b \tag{3}$$

The thermal efficiency, η_{th}, is the ratio of the useful heat to the solar energy:

$$\eta_{th} = \frac{Q_u}{Q_s} \tag{4}$$

The useful exergy, Ex_u, product is given:

$$Ex_u = Q_u - \dot{m}c_p T_{am} \ln\left[\frac{T_{out}}{T_{in}}\right] - \dot{m}T_{am}\frac{\Delta P}{\rho_f T_{fm}} \tag{5}$$

The first term of the eq. (5) is the useful energy production, the second term indicates the irreversibility due to the temperature increase and the third term indicates the irreversibility due to the pressure drop.

The exergy flow of the solar irradiation, Ex_s, is calculated using the Petela model [26]:

$$Ex_s = Q_s\left[1 - \frac{4}{3}\left(\frac{T_{am}}{T_{Sun}}\right) + \frac{1}{3}\left(\frac{T_{am}}{T_{Sun}}\right)^4\right] \tag{6}$$

The Petela model is a suitable model for the solar beam irradiation which is close to the undiluted solar irradiation. The Sun temperature, T_{Sun}, can be taken equal to 5770 K in eq. (6). It is important to state that the temperature levels in eqs. (5) and (6) have to be in Kelvin units.

The exergy efficiency, η_{ex}, is the ratio of the useful heat to the solar energy:

$$\eta_{ex} = \frac{Ex_u}{Ex_s} \tag{7}$$

The daily quantities are calculated using the integration during the day duration, *N*. Below, all the utilized daily energy quantities are given:

– daily useful energy production

$$D_u = \int_{t=0}^{t=N} Q_u \mathrm{d}t \tag{8}$$

– daily incident solar energy

$$D_s = \int_{t=0}^{t=N} Q_s \mathrm{d}t \tag{9}$$

– daily useful exergy production

$$Z_u = \int_{t=0}^{t=N} Ex_u \mathrm{d}t \tag{10}$$

– daily incident solar exergy

$$Z_s = \int_{t=0}^{t=N} Ex_s \mathrm{d}t \tag{11}$$

– the daily thermal efficiency, $\eta_{th,d}$ is defined

$$\eta_{th,d} = \frac{D_u}{D_s} \tag{12}$$

– the daily exergy efficiency, $\eta_{ex,d}$ is defined

$$\eta_{ex,d} = \frac{Z_u}{Z_s} \tag{13}$$

Results

Preliminary calculations

The first part of the present study is associated with the determination of the flow rate in the system. Figure 2 depicts the system thermal performance under different flow rates from 50 L per minute up to 300 L per minute. These results are given for three inlet temperature levels (100 °C, 200 °C, and 300 °C), for direct beam irradiation equal to 100 W/m^2 and 25 °C ambient temperature. It is obvious that higher flow rate leads to higher thermal efficiency. Higher flow rate makes the flow more turbulent and so the heat transfer between the fluid and the receiver is reduced. This result makes the receiver to be colder and to have lower thermal losses and the fact that increases the thermal efficiency. It is obvious that after 250-300 L per minute, the curves tend towards to horizontal for all the examined temperatures. Moreover, extremely high flow rate leads to higher pressure drop and consequently to higher pumping work demand. So, the value of 300 L per minute is selected as one reliable choice for this study. This flow rate is selected for all the following study.

Figure 3 illustrates the thermal and exergy efficiency of the collector for different inlet temperatures from 25 °C up to 325 °C with a flow rate equal to 300 L per minute. Higher inlet temperature leads to lower thermal efficiency because higher temperature levels are associated with higher thermal losses. The exergy efficiency has an increasing rate with the increase of the inlet temperature. This result is explained by the higher exergy efficiency factor $(1 - T_{am}/T_{fm})$ with the temperature increase.

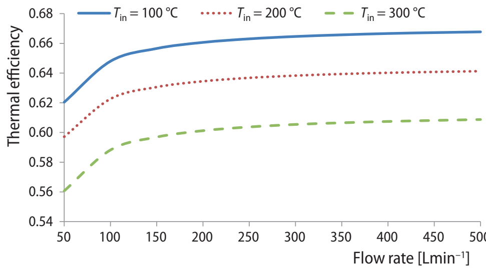

Figure 2. The impact of the flow rate on the thermal efficiency (G_b = 1000 W/m^2 and T_{am} = 25 °C)

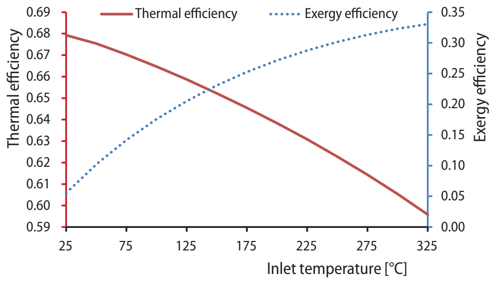

Figure 3. The impact of the temperature in the thermal and exergy efficiency (G_b = 1000 W/m^2, T_{am} = 25°C, and V = 300 L/min)

Daily performance results

The next step in this work is the presentation of the collector daily performance. A typical sunny day is selected from the [27]. The direct solar beam irradiation (DNI) and the ambient temperature of this day are depicted in fig. 4.

Figures 5-9 exhibits the collector thermal and exergy performance. The flow rate is 300 L per minute for all the cases, while it has assumed constant daily inlet temperature in order to simplify the calculations. The inlet temperature level is examined parametrically in these figures.

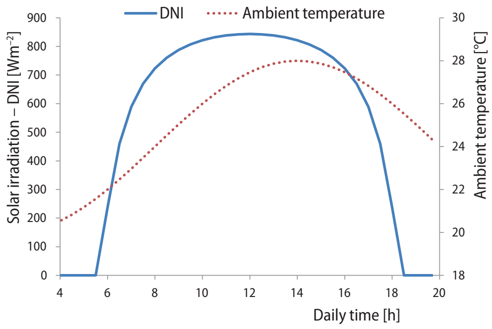

Figure 4. The weather data of the examined day

Figure 5 depicts the thermal production, the exergy production, the thermal efficiency and the exergy efficiency for inlet temperature equal to 200 °C (a typical value for medium temperature applications). It is obvious that both thermal and exergy productions follow the solar irradiation trends of fig. 4 and they are maximized at solar noon (12:00). The thermal production is 5474 W and the exergy 2117 W. The thermal efficiency is approximately constant during the day and it is about 63%, while the exergy efficiency is also approximately constant and close to 26%.

Figures 6-9 illustrate the useful production, the exergy production, the thermal efficiency and the exergy efficiency respectively for three inlet temperature levels (100 °C, 200 °C and 300 °C). The thermal efficiency is higher for lower inlet temperatures according to fig. 6 while the exergy efficiency is higher for higher inlet temperatures according to fig. 7. The important conclusion from these figures is that the thermal efficiency curves are close to each other while the exergy curves are not so close. This result proves that the inlet temperature has a higher impact on the exergy performance than in the thermal performance.

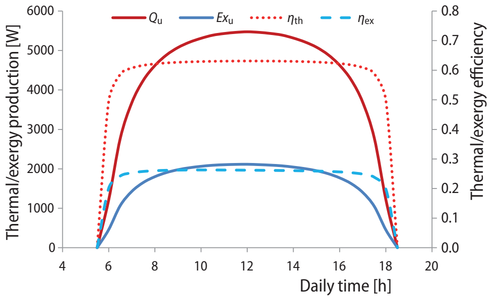

Figure 5. Thermal and exergy production efficiency of the examined day with inlet temperature equal to 200 °C

The thermal efficiency is depicted in fig. 8 and the exergy in fig. 9. The thermal efficiency is approximately symmetrical to the solar noon. On the other hand, the exergy efficiency is not symmetrical because of the impact of the ambient temperature on the results. After the solar noon, the ambient temperature has an increasing rate, fig. 4, and this fact reduces the exergy factor $(1 - T_{am}/T_{fm})$. This reduction is not so high but it is worthy to discuss it. Another important conclusion from figs. 8 and 9 is that both thermal and exergy efficiencies are approximately constant for the greatest duration of the day. This fact proves that the solar irradiation level and the ambient temperatures have only a small impact on the system performance. On the other hand, the inlet temperature has a higher impact on the performance and especially in the exergy performance.

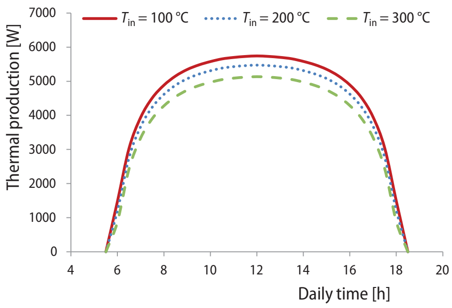

Figure 6. Thermal production of three inlet temperatures

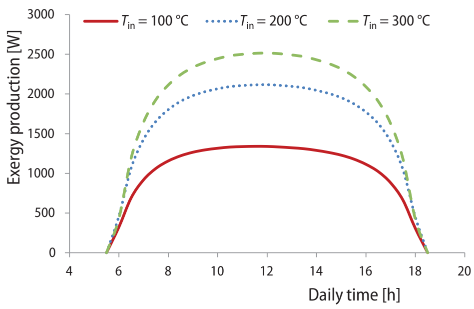

Figure 7. Exergy production of three inlet temperatures

At the end of this section, tab. 1 includes the daily results of the system for different inlet temperatures from 50 °C up to 350 °C with step 50 °C. The thermal efficiency is found to be ranged from 54.65% for 350°C up to 67.36% for 50 °C, while the exergy efficiency from 8.77% for 50 °C up to 31.07% for 350 °C. The useful heat production is ranged from 50 kWh to 61 kWh while the exergy from 7 kWh to 26 kWh. The solar energy and exergy are constant for all the examined cases and they are about 90 kWh and 84 kWh, respectively.

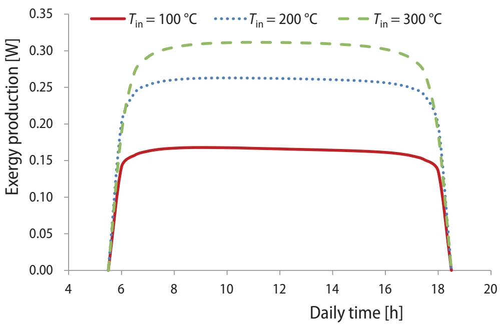

Figure 8. Thermal efficiency for three inlet temperatures

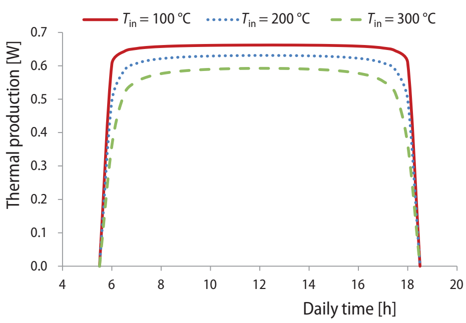

Figure 9. Exergy efficiency for three inlet temperatures

Table 1. Daily performance results for the examined inlet temperatures

T_{in}	D_u	Z_u	D_s	Z_s	$\eta_{th,d}$	$\eta_{ex,d}$
[°C]	[kWh]	[kWh]	[kWh]	[kWh]	[–]	[–]
50	60880	7374	90373	84120	67.36%	8.77%
100	59437	13756	90373	84120	65.77%	16.35%
150	57830	18349	90373	84120	63.99%	21.81%
200	56046	21641	90373	84120	62.02%	25.73%
250	54070	23922	90373	84120	59.83%	28.44%
300	51863	25382	90373	84120	57.39%	30.17%
350	49387	26133	90373	84120	54.65%	31.07%

Conclusions

In this work, the daily performance of a solar dish collector is examined under different inlet temperatures. The analysis is performed using a developed numerical module in EES for a real solar dish collector with an improved reflective material. The optical efficiency of the improved system is 69%, a satisfying value. The most important conclusions of this work are listed as follows.

- The flow rate of 300 L per minute is found to be a suitable choice in order to achieve adequate thermal efficiency.
- The thermal and the exergy efficiency are found to be approximately constant during the daily operation. The inlet temperature is found to be the most important parameter on the collector performance.
- The daily thermal efficiency is found to be ranged from 54.65% up to 65.77% with respective useful heat production from 49.4 kW up to 60.9 kW.
- The daily exergy efficiency is found to be ranged from 8.77% up to 31.07% with respective exergy production from 7.4 kW up to 26.1 kW.
- Higher inlet temperature leads to lower thermal efficiency and higher exergy efficiency on a daily basis.
- The obtained results indicate that the present improved system can produce high amounts of energy and exergy on a daily basis.

Nomenclature

A_a – collecting area, [m^2]
c_p – specific heat capacity under constant pressure, [Jkg^{-1}K^{-1}]
D – daily energy production, [kWh]
DNI – direct beam solar irradiation, [Wm^{-2}]
Ex – exergy flow, [W]
G_b – solar beam irradiation, [Wm^{-2}]
$\dot{m}$ – mass-flow rate, [kgs^{-1}]
N – day duration, [h]
ΔP – pressure drop, [Pa]
Q – heat transfer rate, [W]
T – temperature, [°C]
t – time, [h]
V – volumetric flow rate, [Lh^{-1}]
Z – daily exergy production, [kWh]

Greek symbols

α – absorbance, [–]
γ – intercept factor, [–]
η – efficiency, [–]
ρ – reflectance, [–]
ρ_f – fluid density, [kgm^{-3}]

Subscripts and superscripts

am – ambient
d – daily
ex – exergetic
fm – cooling fluid
in – inlet
opt – optical
out – outlet

s – solar
th – thermal
u – useful
0 – reference

Acronyms

EES – engineering equator solver
PMMA – polymethyl methacrylate

References

[1] Ferreira, A. C., *et al.*, Design of a Solar Dish Stirling Cogeneration System: Application of a Multi-Objective Optimization Approach, *Applied Thermal Engineering, 123* (2017), Aug., pp. 646-657
[2] Allouhi, A., *et al.*, Yearly Performance of Low-Enthalpy Parabolic Trough Collectors in Mena Region According to Different Sun-Tracking Strategies, *Applied Thermal Engineering, 128* (2018), Jan., pp. 1404-1419
[3] Moradi, M., Mehrpooya, M., Optimal Design and Economic Analysis of a Hybrid Solid Oxide Fuel Cell and Parabolic Solar Dish Collector, Combined Cooling, Heating and Power (CCHP) System Used For a Large Commercial Tower, *Energy, 130* (2017), July, pp. 530-543
[4] Bellos, E., *et al.*, Energetic, Exergetic and Financial Evaluation of a Solar Driven Absorption Chiller – A Dynamic Approach, *Energy Conversion and Management, 137* (2017), Apr., pp. 34-48
[5] Loni, R., *et al.*, Performance Study of a Solar-Assisted Organic Rankine Cycle Using a Dish-Mounted Rectangular-Cavity Tubular Solar Receiver, *Applied Thermal Engineering, 108* (2016), Sept., pp. 1298-1309
[6] Loni, R., *et al.*, Optimizing the Efficiency of a Solar Receiver with Tubular Cylindrical Cavity for a Solar-Powered Organic Rankine Cycle, *Energy*, *112* (2016), Oct., pp. 1259-1272
[7] Zou, C., *et al.*, Design and Optimization of a High-Temperature Cavity Receiver for a Solar Energy Cascade Utilization System, *Renewable Energy, 103* (2017), Apr., pp. 478-489
[8] Mawire, A., Taole, S. H., Experimental Energy and Exergy Performance of a Solar Receiver for a Domestic Parabolic Dish Concentrator for Teaching Purposes, *Energy for Sustainable Development, 19* (2014), Apr., pp. 162-169
[9] Loni, R., *et al.*, Thermodynamic Analysis of an Organic Rankine Cycle Using a Tubular Solar Cavity Receiver, *Energy Conversion and Management, 127* (2016), Nov., pp. 494-503
[10] Loni, R., *et al.*, Numerical and Experimental Investigation of Wind Effect on a Hemispherical Cavity Receiver, *Applied Thermal Engineering, 126* (2017), Nov., pp. 179-193
[11] Xu, G., *et al.*, Design and Characteristics of a Novel Tapered Tube Bundle Receiver for High-Temperature Solar Dish System, *Applied Thermal Engineering, 91* (2015), Dec., pp. 791-799
[12] Zhu, J., *et al.*, Experimental Study of the Energy and Exergy Performance for a Pressurized Volumetric Solar Receiver, *Applied Thermal Engineering, 104* (2016), July, pp. 212-221
[13] Daabo, A. M., *et al.*, The Optical Efficiency of Three Different Geometries of a Small Scale Cavity Receiver for Concentrated Solar Applications, *Applied Energy, 179* (2016), Oct., pp. 1081-1096
[14] Loni, R., *et al.*, Exergy Analysis of a Solar Organic Rankine Cycle with Square Prismatic Cavity Receiver, *International Journal of Exergy, 22* (2017), 2, pp. 103-124
[15] Loni, R., *et al.*, Thermodynamic Analysis of a Solar Dish Receiver Using Different Nanofluids, *Energy, 133* (2017), Aug., pp. 749-760
[16] Loni, R., *et al.*, ANN Model to Predict the Performance of Parabolic Dish Collector with Tubular Cavity Receiver, *Mechanics & Industry, 18* (2017), 4, 408
[17] Pavlovic, S., *et al.*, Experimental and Numerical Investigation on the Optical and Thermal Performance of Solar Parabolic Dish and Corrugated Spiral Cavity Receiver, *Journal of Cleaner Production, 150* (2017), May, pp. 75-92
[18] Pavlovic, S., *et al.*, Experimental Investigation and Parametric Analysis of a Solar Thermal Dish Collector with Spiral Absorber, *Applied Thermal Engineering, 121* (2017), July, pp. 126-135
[19] Stefanovic, V. P., *et al.*, A Detailed Parametric Analysis of a Solar Dish Collector, *Sustainable Energy Technologies and Assessments, 25* (2018), Feb., pp. 99-110
[20] Pavlović, S. R., *et al.*, Optical Analysis and Performance Evaluation of a Solar Parabolic Dish Concentrator, *Thermal Science, 20* (2016), Suppl. 5, pp. S1237-S1249
[21] Pavlovic, S., *et al.*, Exergetic Investigation of a Solar Dish Collector with Smooth and Corrugated Spiral Absorber Operating with Various Nanofluids, *Journal of Cleaner Production, 174* (2018), Feb., pp. 1147-1160
[22] Pavlović, S. R., *et al.*, Design, Simulation and Optimization of a Solar Dish Collector Spiral-Coil Thermal Absorber, *Thermal Sscience, 20* (2016), 4, pp. 1387-1397

[23] ***, http://www.almecogroup.com/en
[24] ***, F-Chart Software, Engineering Equation Solver (EES); 2015. Available at: http://www. fchart.com/ees.
[25] ***, Therminol, Therminol VP-1; 2016. Available at: http://www.therminol.com/pages/bulletins/therminol_VP1.pdf.
[26] Petela, R., Exergy of Undiluted Thermal Radiation, *Solar Energy, 74* (2003), 6, pp. 469-488
[27] Bellos, E., *et al.*, Daily Performance of Parabolic Trough Solar Collectors, *Solar Energy, 158* (2017), Dec., pp. 663-678

Paper submitted: January 24, 2018
Paper revised: February 27, 2018
Paper accepted: February 27, 2018